Metal Chalcogenides

International Edition: DOI: 10.1002/anie.201503353
German Edition: DOI: 10.1002/ange.201503353

# Solution-Phase Conversion of Bulk Metal Oxides to Metal Chalcogenides Using a Simple Thiol–Amine Solvent Mixture**

*Carrie L. McCarthy, David H. Webber, Emily C. Schueller, and Richard L. Brutchey**

***Abstract:*** *A thiol–amine solvent mixture is used to dissolve ten inexpensive bulk oxides ($Cu_2O$, ZnO, $GeO_2$, $As_2O_3$, $Ag_2O$, CdO, SnO, $Sb_2O_3$, PbO, and $Bi_2O_3$) under ambient conditions. Dissolved oxides can be converted to the corresponding sulfides using the thiol as the sulfur source, while selenides and tellurides can be accessed upon mixing with a stoichiometric amount of dissolved selenium or tellurium. The practicality of this method is illustrated by solution depositing $Sb_2Se_3$ thin films from compound inks of dissolved $Sb_2O_3$ and selenium that give high photoelectrochemical current response. The direct band gap of the resulting material can be tuned from 1.2–1.6 eV by modulating the ink formulation to give compositionally controlled $Sb_2Se_{3-x}S_x$ alloys.*

Inexpensive solution processing and deposition of inorganic semiconductors is of great interest for large-scale macroelectronics applications, especially low-temperature methods that are compatible with a wide range of substrates. Solution processing and deposition of inorganic semiconductors has important implications in the areas of photovoltaics,[1] flat panel displays,[2] thermoelectrics,[3] phase change memory,[4] and thin-film transistors;[5] however, direct solution processing of these bulk materials is typically difficult because of their complete insolubility in "normal" solvents. As an exception to this statement, the dissolution of bulk chalcogenide semiconductors to form molecular inks has been most successfully and broadly realized using hydrazine as the solvent, through a process that was developed by Mitzi and co-workers at IBM.[6] In this process, molecular solutes are formed by the reaction of bulk metal chalcogenides with $E^{2-}$ ($E^{2-} = S^{2-}$, $Se^{2-}$, and $Te^{2-}$), where $E^{2-}$ is formed by the in-situ reduction of a stoichiometric amount of chalcogen with hydrazine.

While the dissolution of bulk chalcogenide semiconductors in hydrazine gives molecular inks that can be solution processed into extremely high-quality and functional thin films, the explosive, highly toxic, and carcinogenic properties of hydrazine make it less attractive for scale. Thus, new solvents or solvent mixtures are needed that 1) can dissolve a wide scope of bulk materials, 2) are less hazardous, and 3) have sufficient volatility for solution processing. Toward this goal, we recently reported the remarkable ability of binary alkanethiol–1,2-ethylenediamine (en) solvent mixtures to dissolve bulk gray selenium, tellurium, SnS, and a series of nine $V_2VI_3$ chalcogenides (where V = As, Sb, Bi and VI = S, Se, Te) at room temperature and ambient pressure.[7] This chemistry is inspired by the reaction of sulfur with mixtures of thiols and amines, whereby the thiol is deprotonated and the resulting thiolate, through a series of nucleophilic attacks, opens and comminutes the sulfur ring.[8] This new alkahest (or "universal" solvent) for chalcogenide semiconductors gives stable inks that upon solution deposition and mild thermal annealing regenerate crystalline chalcogenide thin films. Further, this solvent system is also capable of making inks from the reaction of dissolved gray selenium and tellurium with elemental metal(loid)s, such as tin and antimony. In this way, crystalline $Sb_2Se_3$ and SnTe films were prepared when elemental antimony or tin were dissolved in the presence of selenium or tellurium, respectively, and the resulting ink was then subsequently solution deposited and annealed to 250 °C.[7a] Building off this result, Pan et al. used a derivative solvent mixture of thioglycolic acid and ethanolamine to dissolve elemental copper, zinc, and tin together with selenium to form a precursor ink that was used to generate CZTSe thin films for photovoltaics.[9]

While the binary thiol–amine solvent mixture has proven effective for the solution processing of bulk chalcogenide semiconductors, the bulk metal chalcogenide starting materials can be expensive, and the elemental metal(loid) starting materials can have little to no inherent solubility in the absence of dissolved selenium or tellurium.[7a] It is therefore of interest to explore alternate metal containing starting materials that can overcome these issues. Along these lines, the equivalent dissolution of cheap, abundant, and sustainable metal oxide starting materials would be an attractive alternative entrée to semiconductor inks if the corresponding metal chalcogenides could be produced. Herein, we demonstrate the extensive capability of this thiol–en solvent mixture to dissolve ten bulk oxides under ambient conditions. Specific focus is placed on the solution processing of $Sb_2Se_3$ thin films from compound inks of dissolved $Sb_2O_3$ and selenium, and the accessibility of crystalline $Sb_2Se_{3-x}S_x$ solid solutions from these inks, which can be used as a valuable tool in photovoltaic absorber layer band gap engineering.

Inks of ten metal(loid) oxides (i.e., $Cu_2O$, ZnO, $GeO_2$, $As_2O_3$, $Ag_2O$, CdO, SnO, $Sb_2O_3$, PbO, and $Bi_2O_3$) were readily prepared by dissolving the bulk oxide powder in a binary mixture of a thiol (ethanethiol (EtSH), 2-mercaptoethanol

[*] C. L. McCarthy, Dr. D. H. Webber, E. C. Schueller, Prof. R. L. Brutchey
Department of Chemistry, University of Southern California
Los Angeles, CA 90089-0744 (USA)
E-mail: brutchey@usc.edu

[**] This chemistry was developed with funding support from the National Science Foundation under DMR-1205712. C.L.McC. acknowledges support from the Graduate Research Fellowship Program of the National Science Foundation.

Supporting information for this article is available on the WWW under http://dx.doi.org/10.1002/anie.201503353.

  

(Merc), or 1,2-ethanedithiol (EDT)) and en in a 1:4 vol/vol ratio at room temperature and ambient pressure. Solubility limits of the various oxides were determined gravimetrically after 24 h of stirring at room temperature (Table S1 in the Supporting Information). Solubilities of these oxides, expressed as wt% solute in the saturated solution (20–25 °C, 1 atm), range from 5-10 wt% for $Cu_2O$, $GeO_2$, and $As_2O_3$, 10–15 wt% for ZnO and SnO, 15–20 wt% for $Ag_2O$, CdO, $Sb_2O_3$, and $Bi_2O_3$, and 25–30 wt% for PbO. The resulting oxide inks are all optically transparent (Figure 1), and remain stable for periods ranging from days to months.

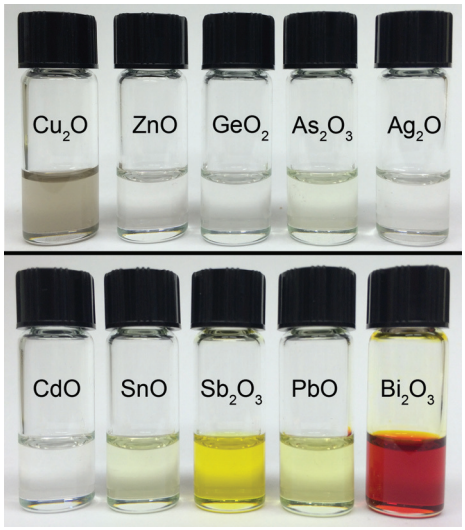


***Figure 1.*** Photograph of dilute (ca. 5 wt%) solutions of ten bulk oxides in a 1:4 vol/vol ethanethiol–1,2-ethylenediamine solvent mixture.

Conversion of the metal(loid) oxide inks into the corresponding metal(loid) sulfides was possible upon mild annealing to 300–375 °C in nearly all cases. Six of the oxide inks studied are converted into their corresponding phase-pure, crystalline sulfide (i.e., ZnS, $Ag_2S$, CdS, SnS, $Sb_2S_3$, and PbS), whereby the alkanethiol in the solvent mixture acts as the sole sulfur source (Figure S2a–f). In some cases, the chemical identity of the alkanethiol has an effect on the crystal structure of the recovered sulfide. For example, while the EtSH-en and Merc-en inks of ZnO and CdO give the corresponding phase-pure cubic sulfides after annealing to 300 °C, the EDT–en inks of these same oxides give a mixture of cubic and hexagonal phases after annealing to the same temperature. This result suggests that the phase of these sulfides can be kinetically influenced depending on the ink formulation.

Mixing the oxide inks with stoichiometric amounts of inks of selenium or tellurium results in one of two scenarios: 1) the mixture remains fully dissolved as an ink (we will refer to this result as a "compound ink"), or 2) a solid precipitates out of solution. Each of the compound inks was thermally decomposed at 300–375 °C after solution deposition, or in the case that a precipitate forms, it was isolated by centrifugation and washed with isopropyl alcohol. It was found that phase-pure, crystalline $Ag_2Se$, $Ag_2Te$, and PbTe were all recoverable by direct precipitation out of solution at room temperature, while phase-pure $Cu_2Se$, ZnSe, CdSe, and $Sb_2Se_3$ were recoverable from the corresponding compound inks via solution deposition and annealing (Figure S2 g–m). Sulfur volatilizes at a lower temperature than selenium, and it is likely that this volatility difference between sulfur and selenium plays a role in the conversion to selenides upon annealing rather than sulfides.[6b,10]

The prospective use of the compound inks to prepare binary and ternary chalcogenide semiconductors will now be explored in more detail using $Sb_2Se_3$ as a model system. In recent years, both $Sb_2S_3$ and $Sb_2Se_3$ have been explored as thin film absorbers for photovoltaic devices due to their near optimal direct band gaps of 1.7–1.1 eV, high absorption coefficients in the visible region ($\alpha = 10^5\ cm^{-1}$), and the fact that they are comprised of relatively earth abundant elements.[11] To demonstrate the utility of the compound inks, inks of $Sb_2O_3$ and selenium in EtSH-en were combined in a 1:3 stoichiometric ratio and then the compound ink was subsequently spin coated onto glass substrates and annealed to 350 °C to give nearly opaque dark gray films of crystalline $Sb_2Se_3$ (Figure 2 a). Thermogravimetric analysis (TGA) was used to determine the temperature needed to decompose the compound ink and convert it to $Sb_2Se_3$. After drying the compound ink to 125 °C, the sample displayed a multistep mass loss of ca. 65 wt% by TGA with an end point of decomposition observed at 300 °C (Figure S3). FT-IR spectroscopy corroborated the loss of organics after annealing to 300 °C, as evidenced by the complete loss of strong $\nu$(N-H) and $\nu$(C-H) stretching bands originating from the solvent mixture (Figure S4). Powder X-ray diffraction (XRD) con-

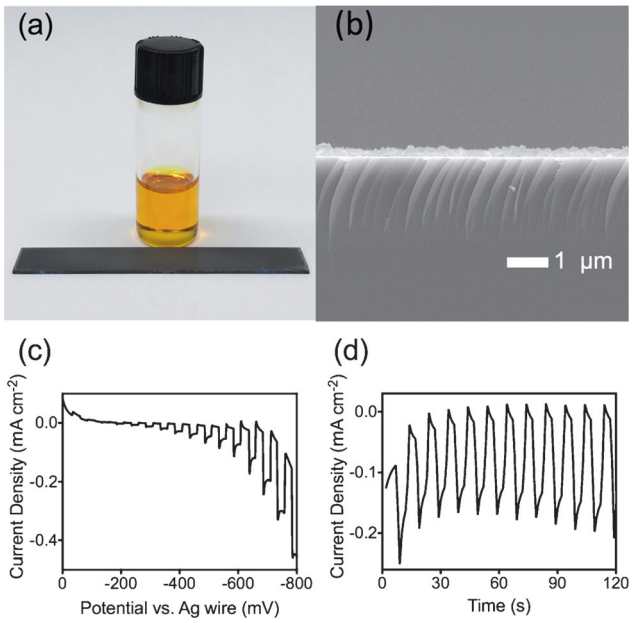


***Figure 2.*** a) Dissolved $Sb_2O_3$ and selenium in EtSH–en and a $Sb_2Se_3$ film on a glass substrate. b) Cross-sectional SEM micrograph of a $Sb_2Se_3$ thin film on glass. c) Linear voltage sweep of p-type $Sb_2Se_3$ with chopped 1-Sun simulated illumination in contact with 0.1 M $Eu(NO_3)_3$(aq), and d) transient photoresponse of $Sb_2Se_3$ under potential control at −700 mV versus Ag wire.

  

firmed that the films were crystalline and phase-pure orthorhombic *Pbnm* $Sb_2Se_3$ (Figure S2k), and bands characteristic of the orthorhombic structure at 84 (translation), 118 (Se-Sb-Se bending), 190 (Se-Sb-Se bending), and 253 $cm^{-1}$ (Sb-Se stretching) were observed by Raman spectroscopy (Figure S5).[12] Inductively coupled plasma optical emission spectroscopy (ICP-OES) confirmed that the material possessed a Sb/Se ratio of ca. 0.65, as expected for a near-stoichiometric material without significant oxide incorporation. This was corroborated by X-ray photoelectron spectroscopy (XPS) data (Figure S7), which shows only one chemical environment for antimony, and no evidence of an O1s peak, indicating that the material is $Sb_2Se_3$ without significant oxide impurities.

Scanning electron microscopy (SEM) images showed that the $Sb_2Se_3$ films were ca. 340 nm thick with a polycrystalline morphology (Figure 2b). The optical band gap of the $Sb_2Se_3$ film was estimated by diffuse reflectance UV/vis spectroscopy using an integrating sphere. Tauc plots suggest that the $Sb_2Se_3$ films possess a direct optical band gap transition of 1.22 eV (i.e., $(F(R)\cdot h\nu)^2$ versus $h\nu$), which is commensurate with values reported for the bulk material.[11] Photoelectrochemical (PEC) experiments were conducted on the $Sb_2Se_3$ thin films as an indication of how the material might perform in solar energy conversion applications. The transient photocurrent response was measured with the $Sb_2Se_3$ films in contact with 0.1M $Eu(NO_3)_3$(aq) as the redox mediator, and a calibrated xenon arc lamp was cycled on and off at regular time intervals to provide 1-Sun chopped illumination. As shown in Figure 2c, the films clearly give cathodic photocurrent that increases as the potential is swept to values negative of −200 mV vs Ag wire, signifying that they demonstrate p-type behavior. DC potential amperometry gave photocurrents $>130\ \mu A\,cm^{-2}$ at an applied bias of −700 mV vs Ag wire under 1-Sun illumination (Figure 2d).

The ability to engineer band gap energies of inorganic semiconductors is important for photovoltaic applications, where the band gap energy of the absorber material can be optimized to match the peak flux of the solar spectrum.[13] It is possible to engineer the band gap of a material by creating a solid solution between two isostructural semiconductors having different band gaps. Solid solutions of $Sb_2Se_{3-x}S_x$ thin films have been previously synthesized by selenization of $Sb_2S_3$, chemical bath deposition, atomic layer deposition, and thermal evaporation;[14] however, all of these methods require energy intensive (high vacuum) or complex and exacting (precise control over temperature, solution pH, etc.) conditions for thin film deposition. We prepared five nominal compositions of $Sb_2Se_{3-x}S_x$ alloys by mixing the $Sb_2O_3$ and selenium inks in alkanethiol–en solvent mixtures in varying Sb/Se stoichiometric ratios. After annealing to 435 °C, crystalline and phase-pure $Sb_2Se_{3-x}S_x$ alloys ($x = 3$, 2.25, 1.50, 0.75, and 0) were recovered. The actual elemental composition of each alloy matched the nominal composition, within experimental error, as determined by ICP-OES. The powder XRD patterns for the end members ($x = 3$ and 0) can be indexed to the orthorhombic *Pbnm* patterns of crystalline $Sb_2S_3$ and $Sb_2Se_3$ (PDF# 00-042-1393 and 01-072-1184, respectively) (Figure 3a). The $Sb_2Se_{3-x}S_x$ alloys display the same overall

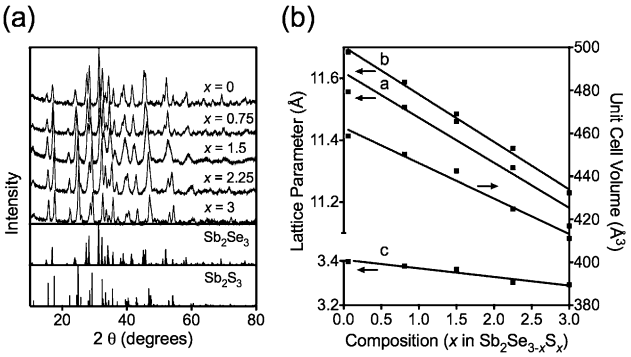


***Figure 3.*** a) Powder XRD patterns of five compositions of $Sb_2Se_{3-x}S_x$ alloys. b) Lattice parameters and unit cell volumes of the five solid solutions showing a linear dependence of unit cell volume on composition.

diffraction patterns as the $Sb_2S_3$ and $Sb_2Se_3$ end-members, indicating they are isostructural with the *Pbnm* crystal structure. As expected for the smaller anionic radius of $S^{2-}$ (Shannon–Prewitt anionic radii of $S^{2-}$ and $Se^{2-}$ are 1.84 and 1.98 Å,[15] respectively), a gradual shift to higher $2\theta$ was observed as the sulfur content in the $Sb_2Se_{3-x}S_x$ alloys increased. The measured unit cell volume demonstrates a linear dependence on the experimentally determined elemental composition (Figure 3b), as it decreases monotonically with increasing sulfur content. This linear dependence is consistent with Vegard's law and demonstrates the compositional homogeneity of these $Sb_2Se_{3-x}S_x$ alloys.

The band gap energies of the alloys also vary as a function of $Sb_2Se_{3-x}S_x$ alloy composition, which can be easily controlled with the compound ink formulation. Tauc plots for the direct optical band gaps derived from UV/vis diffuse reflectance spectra for each of the five nominal compositions of $Sb_2Se_{3-x}S_x$ ($x = 3$, 2.25, 1.50, 0.75, and 0), as well as bulk $Sb_2S_3$ and $Sb_2Se_3$ powders, are given in Figure 4. There is an obvious systematic increase in band gap energy as the nominal sulfur content increases (1.22, 1.27, 1.33, 1.52, and 1.63 eV for $x = 0$, 0.75, 1.5, 2.25, and 3, respectively). As has been shown

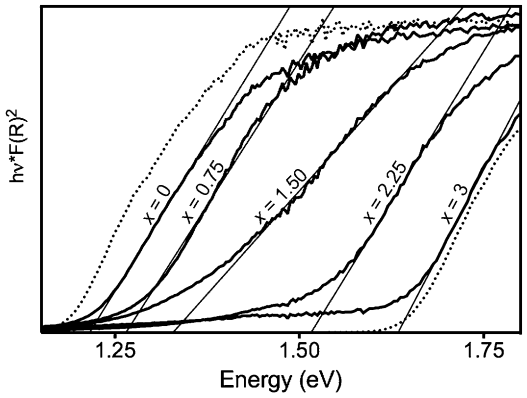


***Figure 4.*** Tauc plots showing band gap tunablity of five $Sb_2Se_{3-x}S_x$ alloy compositions as measured by UV/vis diffuse reflectance spectroscopy. The dotted traces correspond to as-bought bulk $Sb_2Se_3$ ($E_g = 1.2$ eV) and $Sb_2S_3$ ($E_g = 1.6$ eV) powders. The alloys possess direct band baps of 1.63, 1.52, 1.33, 1.27, 1.22 eV for nominal $x = 3$, 2.25, 1.5, 0.75, and 0 compositions, respectively.

  

previously for $Sb_2Se_{3-x}S_x$ solid solutions,[16] the change in direct band gap follows a quadratic dependence on composition of selenium, following the equation $E_{g,dir.}(x) = 0.03175x^2 + 0.04743x + 1.216$ for $Sb_2Se_{3-x}S_x$ (Figure S6). This band gap tunability from 1.2–1.6 eV demonstrates how easily the compound alkanethiol–en inks can be utilized to control chalcogenide semiconductor composition and engineer the resulting band gaps.

In conclusion, we have demonstrated the ability of the thiol–en solvent system to readily dissolve ten bulk metal-(loid) oxides under ambient conditions. From these ten inks, six crystalline sulfides (ZnS, $Ag_2S$, CdS, SnS, $Sb_2S_3$, and PbS) can be recovered upon mild annealing. The oxide inks may also be stoichiometrically mixed with dissolved selenium or tellurium to give compound inks that yield crystalline $Cu_2Se$, ZnSe, CdSe, and $Sb_2Se_3$ upon annealing, while PbTe, $Ag_2Se$, and $Ag_2Te$ can be isolated as phase-pure precipitates at room temperature. The compound ink of dissolved $Sb_2O_3$ and selenium in EtSH-en can be used to spin coat $Sb_2Se_3$ thin films that give strong photocurrent under 1-Sun illumination, thus highlighting the potential of $Sb_2Se_3$ thin films processed from this solvent system for solar energy-conversion applications. Moreover, homogeneous solid solutions of $Sb_2Se_{3-x}S_x$ were readily made from compositionally tailored compound inks with varying Sb/Se ratios, allowing the direct optical band gap to be tuned with increasing selenium content from 1.6–1.2 eV. Given these results, we believe this alkanethiol–en solvent system holds considerable potential for the solution conversion of cheap oxide starting materials to compositionally controlled chalcogenide semiconductors.

**Keywords:** metal chalcogenides · photoelectrochemistry · semiconductors · solution processing · thin films

**How to cite:** *Angew. Chem. Int. Ed.* **2015**, *54*, 8378–8381
*Angew. Chem.* **2015**, *127*, 8498–8501

[1] a) Y. C. Choi, D. U. Lee, J. H. Noh, E. K. Kim, S. I. Seok, *Adv. Funct. Mater.* **2014**, *24*, 3587–3592; b) T. K. Todorov, O. Gunawan, T. Gokmen, D. B. Mitzi, *Prog. Photovoltaics: Res. Appl.* **2013**, *21*, 82–87; c) H. Zhou, Q. Chen, G. Li, S. Luo, T. Song, H. Duan, Z. Hong, J. You, Y. Liu, Y. Yang, *Science* **2014**, *345*, 542–546.

[2] R. H. Reuss, B. R. Chalamala in *Solution Processing of Inorganic Materials* (Ed.: D. B. Mitzi), Wiley, New York **2009**, pp. 1–32.

[3] R. Y. Wang, J. P. Feser, X. Gu, K. M. Yu, R. A. Segalman, A. Majumdar, D. J. Milliron, J. J. Urban, *Chem. Mater.* **2010**, *22*, 1943–1945.

[4] D. J. Milliron, S. Raoux, R. M. Shelby, J. Jordan-Sweet, *Nat. Mater.* **2007**, *6*, 352–356.

[5] D. J. Milliron, D. B. Mitzi, M. Copel, C. E. Murray, *Chem. Mater.* **2006**, *18*, 587–590.

[6] a) D. B. Mitzi, L. L. Kosbar, C. E. Murray, M. Copel, A. Afzali, *Nature* **2004**, *428*, 299–303; b) D. B. Mitzi, *Adv. Mater.* **2009**, *21*, 3141–3158; c) M. Yuan, D. B. Mitzi, *Dalton Trans.* **2009**, 6078–6088.

[7] a) D. H. Webber, J. J. Buckley, P. D. Antunez, R. L. Brutchey, *Chem. Sci.* **2014**, *5*, 2498–2502; b) P. D. Antunez, D. A. Torelli, F. Yang, F. A. Rabuffetti, N. S. Lewis, R. L. Brutchey, *Chem. Mater.* **2014**, *26*, 5444–5446; c) D. H. Webber, R. L. Brutchey, *J. Am. Chem. Soc.* **2013**, *135*, 15722–15725; d) J. J. Buckley, M. J. Greaney, R. L. Brutchey, *Chem. Mater.* **2014**, *26*, 6311–6317.

[8] B. D. Vineyard, *J. Org. Chem.* **1967**, *32*, 3833–3836.

[9] Y. Yang, G. Wang, W. Zhao, Q. Tian, L. Huang, D. Pan, *ACS Appl. Mater. Interfaces* **2015**, *7*, 460–464.

[10] *CRC Handbook of Chemistry and Physics*, 95th ed, CRC, Boca Raton, **2015**.

[11] a) Y. C. Choi, Y. H. Lee, S. H. Im, J. H. Noh, T. N. Mandal, W. S. Yang, S. I. Seok, *Adv. Energy Mater.* **2014**, *4*, 1301680; b) Y. Zhou, M. Leng, Z. Xia, J. Zhong, H. Song, X. Liu, B. Yang, J. Zhang, J. Chen, K. Zhou, J. Han, Y. Cheng, J. Tang, *Adv. Energy Mater.* **2014**, *4*, 1301846; c) Y. C. Choi, D. U. Lee, J. H. Noh, E. K. Kim, S. I. Seok, *Adv. Funct. Mater.* **2014**, *24*, 3587–3592.

[12] I. Efthimiopoulos, J. Zhang, M. Kucway, C. Park, R. C. Ewing, Y. Wang, *Sci. Rep.* **2013**, *3*, 2665–2673.

[13] W. Shockley, H. J. Queisser, *J. Appl. Phys.* **1961**, *32*, 510–519.

[14] a) D. Y. Suárez-Sandoval, M. T. S. Nair, P. K. Nair, *J. Electrochem. Soc.* **2006**, *153*, C91–C96; b) M. Calixto-Rodriguez, H. M. Garcia, M. T. S. Nair, P. K. Nair, *ECS J. Solid State Sci. Technol.* **2013**, *2*, Q69–Q73; c) R. B. Yang, J. Bachmann, E. Pippel, A. Berger, J. Woltersdorf, U. Gosele, K. Nielsch, *Adv. Mater.* **2009**, *21*, 3170–3174; d) E. El-Sayad, *J. Non-Cryst. Solids* **2008**, *354*, 3806–3811.

[15] M. Ladd, *Symmetry of Crystals and Molecules, Vol. 1*, Oxford University Press, New York, **2014**, p. 45.

[16] Z. Deng, M. Mansuripur, A. J. Muscat, *Nano Lett.* **2009**, *9*, 2015–2020.

Received: April 13, 2015
Published online: June 2, 2015

  